Received: 26 October 2023 | Revised: 10 January 2024 | Accepted: 21 January 2024

DOI: 10.1002/app.55250

RESEARCH ARTICLE

Journal of Applied Polymer Science WILEY

Aromatic amino acids as latent, bio-based curing agents and toughening agents for epoxy resins

Florian Rothenhäusler | **Holger Ruckdäschel**

Department of Polymer Engineering, University of Bayreuth, Bayreuth, Germany

Correspondence
Holger Ruckdäschel, Department of Polymer Engineering, University of Bayreuth, Universitätsstraße 30, Bayreuth 95444, Germany.
Email: holger.ruckdaeschel@uni-bayreuth.de

Funding information
Bundesministerium für Wirtschaft und Energie, Grant/Award Number: 20E1907A

Abstract

In the realm of bio-based curing agents, recent investigations have focused on amino acids owing to their distinctive attributes. Nevertheless, the suitability of thermosets cured with aromatic amino acids as latent matrix materials for fiber-reinforced composites remains to be empirically established. Consequently, this study is oriented toward assessing the mechanical properties of diglycidyl ether of bisphenol A when cured with either L-tryptophan or L-tyrosine, in the presence of a latent, urea-based accelerator. The investigated properties include glass transition temperatures, tensile, flexural, compression, and fracture toughness properties. The predominant variations in the mechanical characteristics of these thermosets are confined to their Young's moduli and fracture toughness properties. This divergence is attributed to the greater presence of crystals in the L-tyrosine-cured thermoset, resulting in enhanced reinforcement and toughening effects compared to the L-tryptophan-cured thermoset.

KEYWORDS

amino acid, epoxy resin, fracture toughness, glass transition temperature, mechanical properties, sustainability, tensile strength

1 | INTRODUCTION

Fiber-reinforced epoxy matrix composites play a pivotal role in various industrial sectors, including sports, automotive, wind energy generation, and aerospace applications, thanks to their exceptional combination of high weight-specific strength and modulus.[1,2] Epoxy resins are the preferred choice for pre-impregnated fiber products due to their advantageous attributes, such as significant latency, high mechanical performance, and low viscosity during the fiber impregnation process.[3] It is worth noting that traditional curing agents, such as amines, anhydrides, and phenolic compounds, have been associated with toxic or carcinogenic effects, as documented in prior studies.[4–7]

In contrast to conventional, petroleum-based amine hardeners, amino acids offer a bio-based, non-toxic, and biodegradable alternative.[8–10] Among these, L-tryptophan has garnered considerable attention as a curing agent for epoxy resins, primarily due to the unique structural features of its aromatic side chain, which includes an indolyl group. This structure introduces steric hindrance between cross-links, effectively impeding the rearrangement of network segments. Consequently, this molecular architecture results in a notably elevated glass transition temperature (T_g), as illustrated in Figure 1.

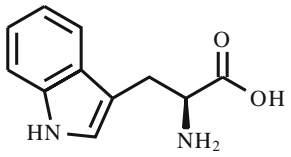

FIGURE 1 Chemical structure of L-tryptophan.

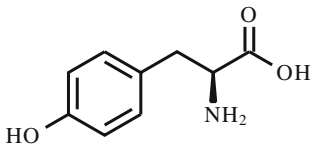

FIGURE 2 Chemical structure of L-tyrosine.

Numerous investigations have been dedicated to studying the reaction kinetics and T_g of diglycidyl ether of bisphenol A (DGEBA) when cured with L-tryptophan.[11–16] Notably, the T_g of the resultant thermoset varies significantly due to differing preparation methods, accelerator types, and the ratio of epoxy resin to L-tryptophan. When ureas are employed as accelerators, the T_g range spans from approximately 66 to 101°C.[14,16] Alternatively, the incorporation of imidazoles as accelerators yields T_g values ranging from roughly 84 to 104°C.[11,13,14]

Albuquerque et al. explored the synergistic effects achieved by employing various amino acids as curing agents for epoxy resins through machine learning. In this context, the T_g of DGEBA cured with L-tryptophan in the presence of a latent, urea-based accelerator was assessed using dynamic mechanical analysis, revealing a T_g of approximately 125°C.[17] Rothenhäusler et al. conducted similar experiments, curing the same resin-curing agent combination alongside the less latent accelerator, 2-ethyl-4-methyl-imidazole.[18] Intriguingly, this alteration led to an increase in T_g to around 138.5°C. This change in T_g is likely attributed to an augmented cross-link density (ν_C), arising from the homopolymerization of DGEBA induced by the imidazole.[19] Notably, the K_{IC} of DGEBA cured with L-tryptophan stands at approximately 1.34 MPa $m^{0.5}$, a notably higher value compared to epoxides cured with dicyandiamide (ranging from 0.6 to 0.7 MPa $m^{0.5}$).[20–22] Furthermore, the fracture energy (G_{IC}) of the L-tryptophan-based thermoset is measured at 575 J m^{-2}, rendering it a compelling material for applications where high toughness is a vital requirement.

In contrast to L-tryptophan, L-tyrosine has received comparatively less attention as a curing agent for epoxy resins. Nonetheless, L-tyrosine holds special significance in the context of curing agents due to the distinctive chemical structure of its side chain, which includes a phenyl group (see Figure 2). Albuquerque et al. observed that when DGEBA is cured with L-tyrosine in the presence of a urea-based accelerator, the resulting material exhibits a T_g of approximately 119°C.[17] Interestingly, the T_g of DGEBA cured with L-tyrosine significantly increases when 2-ethyl-4-methyl-imidazole is utilized as the accelerator. This leads to a thermoset with an impressive T_g of 188°C and a Young's modulus of 3.5 GPa. Notably, these values represent the highest T_g and Young's modulus reported in the literature for an epoxy resin cured with an amino acid.[11–14,16,23–26]

As a response to these considerations, Rothenhäusler and colleagues conducted a comprehensive investigation into the influence of the stoichiometric ratio (R) on the mechanical properties of DGEBA cured with L-tyrosine.[27] Their research revealed that L-tyrosine crystals that are uniformly distributed throughout the cured thermoset grow during the curing of the epoxy resin. The introduction of additional L-tyrosine, signifying R greater than 1, results in an increased quantity of L-tyrosine crystals in the matrix without inducing significant alterations in the network structure of the thermoset. Consequently, the T_g, flexural modulus, flexural strength, and strain at failure exhibit only marginal changes. Moreover, the further addition of L-tyrosine to the matrix leads to an enhanced degree of crystallinity, subsequently resulting in elevated K_{IC} and G_{IC} values. This phenomenon underscores the role of amino acid crystals as effective toughening agents. However, when R is reduced below 1, the flexural modulus decreases and the strain at failure increases. The combined effect of these changes ultimately results in minor modifications in the flexural strength of the thermoset.

In summary, both DGEBA cured with L-tryptophan and DGEBA cured with L-tyrosine demonstrate promise as potential matrix materials for fiber-reinforced composites. However, the existing literature lacks information on the mechanical performance of these resin systems when combined with a latent accelerator. Hence, the primary objective of this study is to comprehensively characterize the T_g, tensile, flexural, compression, and fracture toughness properties of DGEBA cured with either L-tryptophan or L-tyrosine, in conjunction with a latent, urea-based accelerator. Particular emphasis is placed on investigating the role of amino acid crystals as reinforcing agents and modifiers of toughness within the epoxy matrix. The ultimate goal is to ascertain which of the two thermosets is better suited for applications as matrix materials in fiber-reinforced polymers. In continuation of this research, there is an intention to prepare and evaluate natural fiber-reinforced composites employing one of these resin systems, with the results of this forthcoming investigation to be published soon.

2 | EXPERIMENTAL

2.1 | Materials

D.E.R. 331 (epoxide equivalent weight of 187 g mol^{-1}) was procured from Blue Cube Assets GmbH & Co. KG, Olin Epoxy, located in Stade, Germany. The amino acids, L-tryptophan (with a purity 100%) and L-tyrosine, were sourced from Buxtrade GmbH in Buxtehude, Germany. The reaction between these aromatic amino acids and DGEBA is expedited through the addition of the urea-based DYHARD®UR400, which is supplied by Alzchem Group AG, headquartered in Trostberg, Germany.

2.2 | Resin formulation

The DGEBA and amino acid mixtures were prepared via a three-roll milling method outlined in prior studies.[25,26] In this process, it was assumed that L-tryptophan and L-tyrosine possess four and three active hydrogen atoms, respectively.[18] Consequently, the active hydrogen equivalent weights of L-tryptophan and L-tyrosine are determined to be 51.05 and 60.40 g mol^{-1}, respectively. The mixtures are prepared to maintain a R of 1, signifying an equivalence of active hydrogen atoms in the amino acid to epoxy groups in the resin. Subsequently, one weight percentage of DYHARD®UR400 (as detailed in Table 1) is introduced, followed by thorough mixing in a centrifuge speed mixer provided by Hauschild Engineering in Hamm, Germany, operating at 3000 min^{-1} for 120 s. To ensure the removal of any trapped air prior to curing, the mixture is degassed for 60 min at 10 mbar. For the sake of simplicity, the cured thermosets that contain L-tryptophan and L-tyrosine are herein denoted as Tryptopox and Tyropox, respectively, throughout this investigation.

2.3 | Curing cycle and sample preparation

The mixtures comprising epoxy resin, amino acid, and accelerator were poured into pre-heated aluminum molds set at 70°C. These mixtures underwent a curing process lasting 2 h at 120°C and an additional 2 h at 170°C. The curing was carried out within a Memmert ULE 400 convection oven supplied by Memmert GmbH + Co. KG, located in Schwabach, Germany. Following the curing process, the molds were gradually cooled to room temperature over a 3-h duration. Specimens for testing were then prepared from the cured plates in accordance with the relevant ISO standards for each test method. These specimens were created using a Mutronic DIADISC5200 diamond plate saw and CNC milled using a Mutronic Diadrive 2000, both from MUTRONIC Präzisionsgerätebau GmbH & Co. KG, based in Rieden am Forggensee, Germany.

TABLE 1 Compositions of Tryptopox and Tyropox.

Component	Tryptopox	Tyropox
D.E.R. 331	77.8 wt%	74.8 wt%
L-Tryptophan	21.2 wt%	-
L-Tyrosine	-	24.2 wt%
DYHARD®UR400	1 wt%	1 wt%

2.4 | Material characterization

2.4.1 | Differential scanning calorimetry

The determination of the weight fraction of crystalline amino acid, denoted as the degree of crystallinity (X_c), in Tryptopox and Tyropox was carried out through dynamic differential scanning calorimetry (DSC) measurements using a Mettler Toledo DSC 1 instrument (Columbus, Ohio, USA). The amino acids and their corresponding thermosets were subjected to a heating rate of 10 K min^{-1}, increasing the temperature from 25 to 340°C, while maintaining a constant nitrogen flow rate of 50 mL min^{-1} within the sample chamber. The sample masses for the amino acids and thermosets were 0.5 ± 0.25 mg and 7.5 ± 2.5 mg, respectively. The degree of crystallinity (X_c) was calculated as follows:

$$X_c = \frac{H_{\text{Thermoset}}}{H_{\text{AA}}}, \quad (1)$$

where $H_{\text{Thermoset}}$ represents the enthalpy of the cured thermosets, and H_{AA} represents the enthalpy of the amino acid. Three specimens were tested per amino acid and thermoset.

2.4.2 | Dynamic mechanical analysis

Tryptopox and Tyropox underwent dynamic mechanical analysis using a Gabo Eplexor 500 N instrument provided by Gabo Qualimeter Testanlagen GmbH, located in Ahlden, Germany. The testing was performed in tension mode on specimens with dimensions of 50 × 10 × 2 mm^3. The measurements were carried out over a temperature range from −120 to 200°C with a heating rate of 3 K min^{-1}. The tensile force amplitude

and tensile frequency were set to 60 N and 1 Hz, respectively. The T_g was determined as the temperature at which the tangent of the phase angle ($\tan\delta$), reaches its maximum value. To calculate the ν_C of the thermosets, the following formula was employed:

$$\nu_C = \frac{E'}{3RT}, \quad (2)$$

where E' represents the storage modulus at $T = T_g + 50\,K$, and R is the universal gas constant with a value of $8.314\,J\,mol^{-1}\,K^{-1}$.[28] Notably, three specimens were tested for each thermoset to ensure the reliability of the results.

2.4.3 | Tensile tests

The tensile properties of Tryptopox and Tyropox were determined in accordance with DIN EN ISO 527-2 standards. Six 1B dog-bone specimens, each with dimensions of $150 \times 10 \times 4\,mm^3$, were tested. The tests were conducted using a ZwickRoell Z020 universal testing machine supplied by ZwickRoell GmbH & Co. KG in Ulm, Germany. The machine was equipped with a load cell capable of handling loads up to 20 kN. The testing procedure involved a cross-head speed of $5\,mm\,min^{-1}$.

2.4.4 | Three-point bending

The flexural properties of the thermosets, Tryptopox and Tyropox, were assessed in accordance with ISO 178 standards. Ten specimens with dimensions of $80 \times 10 \times 4\,mm^3$ were tested for each material. These tests were conducted on a ZwickRoell Z020 universal testing machine, supplied by ZwickRoell GmbH & Co. KG in Ulm, Germany. The machine was equipped with a load cell capable of accommodating loads up to 20 kN. The testing procedure involved a cross-head speed of $2\,mm\,min^{-1}$.

2.4.5 | Compression tests

The compression strengths of the thermosets, Tryptopox and Tyropox, were examined in compliance with EN ISO 604 standards. Specimens with dimensions of $10 \times 10 \times 4\,mm^3$ were used for these tests. The experiments were conducted on a ZwickRoell Z020 universal testing machine provided by ZwickRoell GmbH & Co. KG in Ulm, Germany. The machine was equipped with a load cell capable of handling loads up to 20 kN. The testing procedure involved a cross-head speed of $1\,mm\,min^{-1}$.

2.4.6 | Fracture toughness

The fracture toughness of Tryptopox and Tyropox was determined following ISO 13586 standards. Eight compact tension specimens were tested using a ZwickRoell Z020 universal testing machine supplied by ZwickRoell GmbH & Co. KG in Ulm, Germany. The machine was equipped with a load cell capable of accommodating loads up to 20 kN. The G_{IC} was calculated using the formula:

$$G_{IC} = \frac{{K_{IC}}^2}{E}(1-\nu^2), \quad (3)$$

where G_{IC} represents the fracture energy, K_{IC} is the critical stress intensity factor in mode I, E is Young's modulus (obtained from the tensile tests), and ν is Poisson's ratio, which is approximately 0.35 in the glassy state of the thermoset.[29]

2.4.7 | Scanning electron microscopy

The fracture surfaces of the compact tension specimens were examined using a Zeiss Gemini 1530 Scanning Electron Microscope, provided by Carl Zeiss AG in Oberkochen, Germany. The analysis was carried out with an acceleration voltage of 3 kV, and the surfaces were coated with a layer of platinum sputtering, with a thickness of approximately 5 nm for enhanced imaging.

3 | RESULTS AND DISCUSSION

3.1 | Differential scanning calorimetry

The outcomes of the dynamic DSC measurements performed on the amino acids and their corresponding thermosets are summarized in Table 2. Notably, the enthalpy values for the amino acids closely align with the findings

TABLE 2 Results of the DSC measurements (average ± standard deviation).

Physical quantity	Tryptopox	Tyropox
$H_{Thermoset}$ in $J\,g^{-1}$	12.4 ± 2.0	72.4 ± 5.8
H_{AA} in $J\,g^{-1}$	375.4 ± 5.6	644.4 ± 4.0
X_c in %	3.3	11.2

of Rodante et al., who reported H_{AA} values of 376.9 J g^{-1} for L-tryptophan and 619.4 J g^{-1} for L-tyrosine.[30] Consequently, the X_c for Tryptopox and Tyropox are estimated to be approximately 3.3% and 11.2%, respectively. These findings are substantiated by SEM images, as discussed in Subsection 3.7. The subsequent sections delve into the implications of the enhanced X_c observed in Tyropox compared to Tryptopox.

3.2 | Dynamic mechanical analysis

Figure 3 displays the storage modulus (E') and tan δ of Tryptopox and Tyropox over a temperature range from −120 to 200°C. At −120°C, the E' of Tryptopox is approximately 4.6 GPa, while Tyropox exhibits a storage modulus of about 6.6 GPa. For a discussion about the differences in Young's moduli of Tryptopox and Tyropox, see Subsection 3.3.

Both Tryptopox and Tyropox exhibit a characteristic peak in their tan δ curves at around −65°C, attributed to the β−relaxation, a typical behavior for DGEBA-type thermosets. This relaxation is commonly associated with the hydroxy ether and diphenyl propane groups present in these materials.[31–33]

As the temperature increases, the E' of the thermosets decrease, reaching values of approximately 2.5 GPa for Tryptopox and 3.2 GPa for Tyropox at room temperature. With further heating up to 100°C, the E' of both thermosets exhibit a gradual decline, but they still remain sufficiently high to ensure the structural integrity of components in potential applications as fiber-reinforced composite matrix materials (see Table 3). Therefore, the upper temperature limit for the service range of both thermosets is around 100°C.

The T_g is indicated by a peak in tan δ at approximately 125°C for both Tryptopox and Tyropox. Notably, in the rubbery state, Tyropox demonstrates a E' roughly five times higher than that of Tryptopox, highlighting the reinforcing effect of amino acid crystals. This substantial difference in storage modulus is a significant factor in why the calculated ν_C cannot be considered representative of the true ν_C of the thermoset. Similar observations were made in previous studies involving epoxy resins cured with amino acids.[27]

At around 200°C, the tan δ of Tryptopox begins to increase, indicating the degradation of L-tryptophan crystals within the thermoset. It is worth noting that a previous investigation studied thermosets composed of DGEBA resin with either L-tryptophan or L-tyrosine, utilizing 2-ethyl-4-methyl-imidazole as an accelerator, which promotes the homo-polymerization of epoxy groups and leads to a higher ν_C.[19] This is why the T_g values of Tryptopox and Tyropox in the present study are lower than those reported in the prior study (138.5 and 188.3°C).[18] Intriguingly, the E' in the present study are less affected by the lower ν_C, underscoring the significant influence of amino acid crystal reinforcement on the thermoset's mechanical properties.

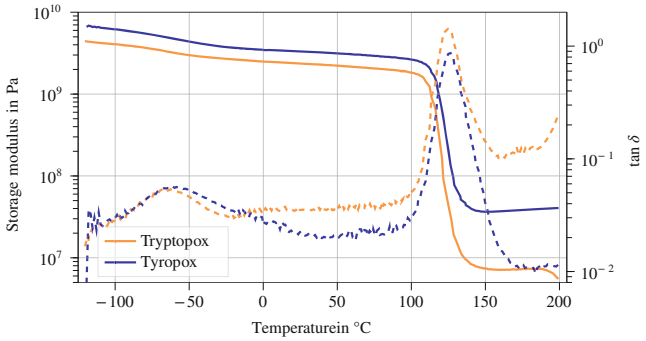

FIGURE 3 Dynamic mechanical analysis of Tryptopox (orange) and Tyropox (blue) between $T = -120$ and 200°C. [Color figure can be viewed at wileyonlinelibrary.com]

TABLE 3 Key data of Tryptopox and Tyropox derived from dynamic mechanical analysis (average ± standard deviation).

Physical quantity	Tryptopox	Tyropox
T_g (max. tan δ) in °C	124.6 ± 0.4	126.1 ± 0.3
Cross-link density ν_C in mol m^{-3}	700 ± 40	3450 ± 55
E' at $T = -120$°C in GPa	4.57 ± 0.10	6.58 ± 0.18
E' at $T = 22$°C in GPa	2.47 ± 0.06	3.24 ± 0.08
E' at $T = 100$°C in GPa	1.89 ± 0.05	2.59 ± 0.05

3.3 | Tensile tests

Figure 4 illustrates the stress–strain curves derived from tensile tests performed on Tryptopox and Tyropox. The Young's modulus of Tryptopox is approximately 2.9 GPa, a value that is noticeably lower than that of Tyropox, which is approximately 3.8 GPa. Amino acid crystals generally possess significantly higher Young's moduli than thermosets at room temperature, making them effective reinforcements in the surrounding thermoset matrix.[34–36] Rothenhäusler et al. demonstrated that the E' increases with an increasing R in DGEBA cured with L-tyrosine.[27] The modulus of L-tyrosine crystals, as determined by Adhikari et al. and Ji et al. using atomic force microscopy nano-indentation, is approximately 42 GPa and 177 GPa, respectively.[37,38] Hence, the difference in Young's moduli between Tryptopox and Tyropox is likely due to variations in the degree of crystallinity (see Section 3.1), crystal morphology, and the distinct elastic properties of the amino acid crystals. In contrast to the Young's moduli of

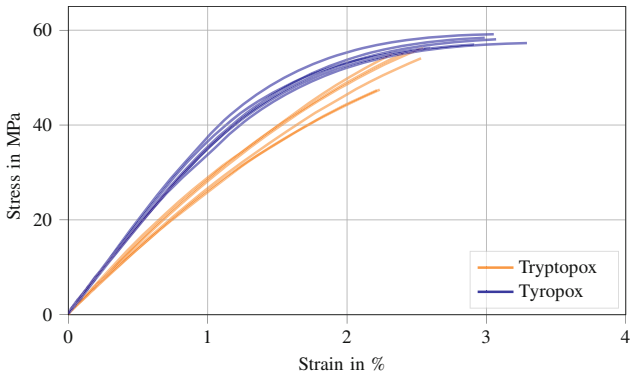

FIGURE 4 Stress–strain curves derived from tensile tests of Tryptopox (orange) and Tyropox (blue). [Color figure can be viewed at wileyonlinelibrary.com]

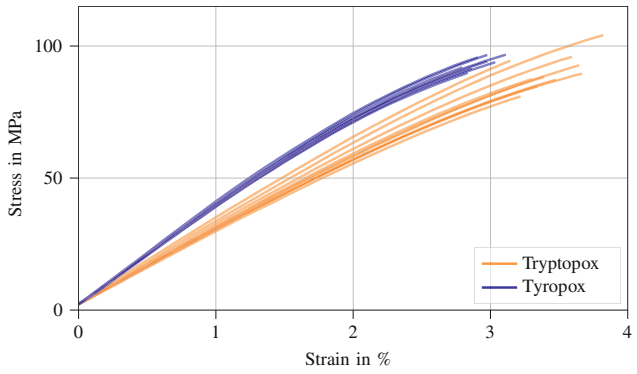

FIGURE 5 Stress–strain curves derived from three-point bending of Tryptopox (orange) and Tyropox (blue). [Color figure can be viewed at wileyonlinelibrary.com]

TABLE 4 Overview of the tensile, flexural, compression and fracture toughness properties of Tryptopox and Tyropox (average ± standard deviation).

	Tryptopox	Tyropox
Tensile modulus in GPa	2.9 ± 0.1	3.8 ± 0.9
Tensile strength in MPa	53 ± 4	58 ± 1
Tensile strain in %	2.4 ± 0.1	3.0 ± 0.2
Flexural modulus in GPa	3.0 ± 0.2	3.7 ± 0.1
Flexural strength in MPa	91 ± 6	94 ± 2
Flexural strain in %	3.5 ± 0.2	3.0 ± 0.1
Compression yield strength in MPa	100 ± 2	106 ± 3
Compression yield strain in %	10.9 ± 0.6	10.1 ± 0.6
K_{IC} in MPa $m^{0.5}$	1.26 ± 0.12	1.91 ± 0.07
G_{IC} in J m^{-2}	451 ± 49	844 ± 58
d_p in µm	16.8	34.6

the thermosets, the tensile strengths of Tryptopox and Tyropox are quite similar, at approximately 53 MPa and 58 MPa, respectively (see Table 4). The stress–strain curves of Tyropox exhibit a more pronounced deviation from linear elastic behavior compared to those of Tryptopox. This suggests that Tyropox begins to deform plastically to a certain extent. Consequently, the tensile strain at failure for Tyropox (3.0%) is higher than that for Tryptopox (2.4%).

3.4 | Three-point bending

Figure 5 displays the stress–strain curves obtained from three-point bending tests conducted on Tryptopox and Tyropox. Consistent with the results of DMA and tensile tests, the flexural modulus of Tyropox (3.7 GPa) is considerably higher than that of Tryptopox (3.0 GPa). In contrast, the flexural strengths of Tryptopox and Tyropox are approximately 91 GPa and 94 GPa, respectively, indicating only slight differences in strength values.

Notably, similar to the tensile tests, the flexural strain at failure for Tyropox (3.0%) is smaller than that of Tryptopox (3.5%). Importantly, both Tryptopox and Tyropox exhibit higher flexural strengths than their counterparts cured in the presence of imidazole.[18] In the prior study, the flexural strengths were approximately 71 MPa for both thermosets, highlighting the advantageous mechanical properties of the current amino acid-cured formulations.

3.5 | Compression tests

Figure 6 presents the stress–strain curves obtained from compression strength tests performed on Tryptopox and Tyropox. In this test, both thermosets exhibit yield behavior under compression stresses of approximately 100 MPa at compression strains of roughly 10% to 11% (see Table 4). Interestingly, in the prior study, the thermoset comprised of DGEBA, L-tyrosine, and imidazole did not display a distinct yield behavior during compression. One possible explanation is that the embrittlement of the thermoset resulting from the homopolymerization of DGEBA, induced by the presence of imidazole, may have prevented the plastic deformation of the material. This difference highlights how the choice of curing agents and accelerators can significantly influence the mechanical behavior of epoxy resins.

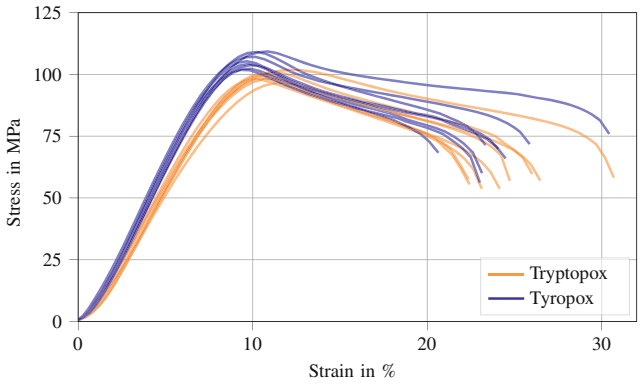

FIGURE 6 Stress–strain curves derived from compression strength tests of Tryptopox (orange) and Tyropox (blue). [Color figure can be viewed at wileyonlinelibrary.com]

3.6 | Fracture toughness

Figure 7 illustrates the critical stress intensity factor in mode I (K_{IC}) and the fracture energy (G_{IC}) of Tryptopox and Tyropox compared to epoxy resins toughened with various toughening agents. Tryptopox and Tyropox exhibit K_{IC} values of about 1.26 and 1.91 MPa m$^{0.5}$, respectively, while their corresponding G_{IC} values are approximately 451 and 844 J m^{-2}, respectively. Naturally, the higher X_c in Tyropox compared to that in Tryptopox increases the thermoset's resistance to crack propagation as well as the energy dissipated during crack growth.

It is important to acknowledge that these values may be significantly underestimated due to the "crack-stopping" effects observed during testing. In conventional brittle materials, loading typically continues until the material's K_{IC} is reached, leading to complete failure of the specimens. Meaning that the material cannot store more internal energy in the form of elastic energy during deformation but rather that energy potential is lowered by creating new surfaces. However, Tryptopox and Tyropox specimens do not fail entirely upon reaching the maximum load (see Figure 8). Instead, the crack is arrested after some distance, likely due to the presence of amino acid crystals, and only continues to grow after an increase in the specimen's load. Since K_{IC} and G_{IC} are both calculated based on the first load peak, they are likely to be highly underestimated because the additional load increase is not considered.

Nevertheless, Tryptopox and Tyropox demonstrate a similar fracture toughness compared to epoxy resins with similar T_g toughened with commercial toughening agents, such as block copolymers and nano-silica particles. This is noteworthy because while there has been extensive research on bio-based epoxy resins and curing agents, fewer investigations have focused on

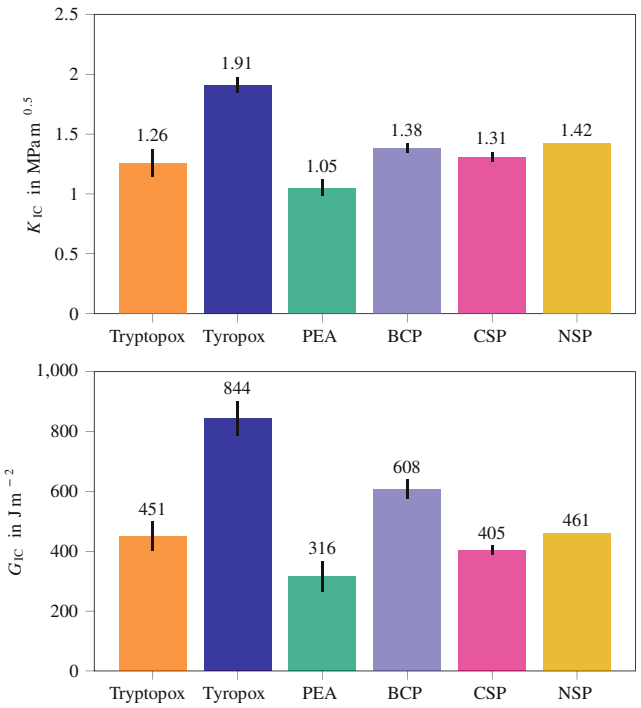

FIGURE 7 Critical stress intensity factor in mode I K_{IC} and fracture energy G_{IC} of Tryptopox (orange) and Tyropox (blue) compared to epoxy resins with similar T_g toughened with polyetheramines (PEA, teal),[39] block copolymers (BCP, purple),[40] core-shell particles (CSP, pink)[40] and nano-silica particles (NSP, yellow).[41] [Color figure can be viewed at wileyonlinelibrary.com]

bio-based toughening agents. Amino acids are unique in that they serve both as curing agents and toughness modifiers. The comparison between the K_{IC} and G_{IC} values of Tyropox and the epoxy resin cured with tyrosine in the presence of an imidazole (0.82 MPa m$^{0.5}$ and 172 J m^{-2}) highlights how the higher network density resulting from the imidazole-induced homo-polymerization makes the thermoset more brittle.[18] Further insights into potential toughening mechanisms are discussed in Section 3.7.

3.7 | Scanning electron microscopy

In Figure 9, the fracture surfaces of compact tension specimens made from Tryptopox and Tyropox are examined at 100, 1000, and 5000× magnification. The fracture surface of Tryptopox appears coarse and contains homogeneously distributed L-tryptophan crystals, which have a distinct plate-like appearance and measure approximately 20 to 100 μm in diameter (see Figure 9a). This plate-like crystal morphology resembles L-tryptophan crystals grown from a solution.[42] In contrast, the fracture

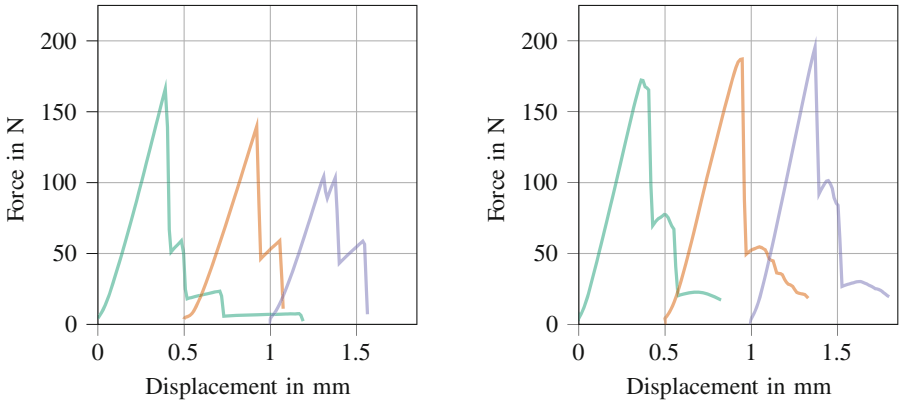

FIGURE 8 Left: Force-displacement curves of compact tension tests of Tryptopox. Right: Force-displacement curves of compact tension tests of Tyropox. [Color figure can be viewed at wileyonlinelibrary.com]

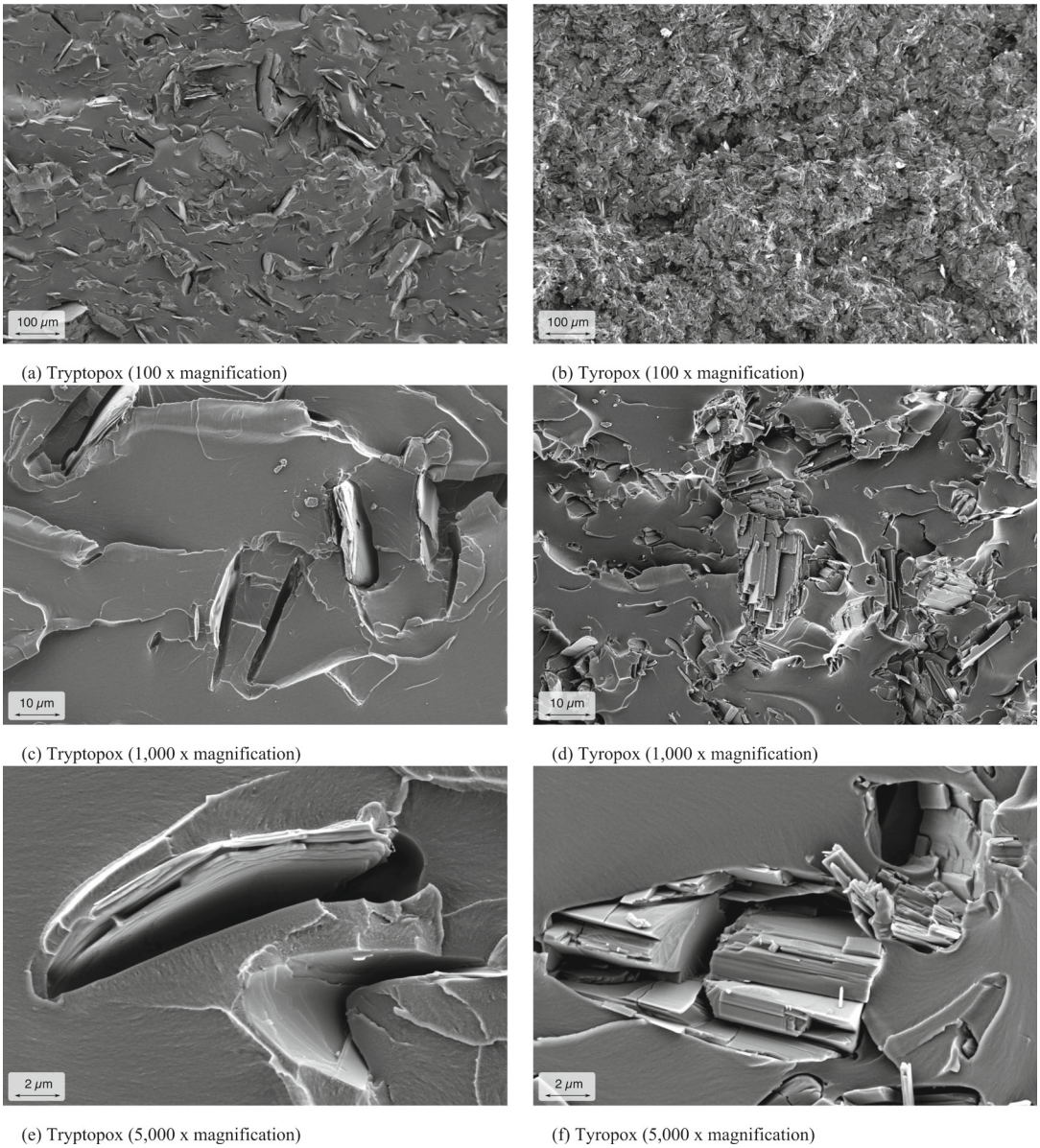

FIGURE 9 Fracture surfaces of compact tension specimens made from Tryptopox and Tyropox at 100, 1000, and 5000× magnification.

surface of Tyropox appears much rougher (see Figure 9b). Comparing both images suggests that there are far fewer crystals in Tryptopox than in Tyropox. The reason for this might be the lower solubility of L-tyrosine in DGEBA compared to that of L-tryptophan. Significant differences in the solubilities of L-tyrosine and L-tryptophan in water have already been widely researched.[43] The low solubility of L-tyrosine is the result of the dimer-formation of L-tyrosine molecules. The carboxylate groups and hydroxyl groups of two adjacent L-tyrosine molecules attract one another, leading to a large building block for L-tyrosine crystals.[38] As a result, L-tyrosine crystals have a higher Young's modulus and thermal stability compared to that of other amino acids.[34–36] Interestingly, the weight proportions of the amino acids in their respective thermosets only differ by about 3 wt% (see Table 1), while the X_c of the thermosets differ by roughly 8%. The lower solubility of L-tyrosine stimulates phase separation and crystal growth within the epoxy matrix. This difference in crystal growth leads to varying degrees of crystallinity and crystal morphology, ultimately affecting the mechanical properties of the thermosets. Nevertheless, both Tryptopox and Tyropox have similar glass transition temperatures.

In Tyropox, rod-shaped L-tyrosine crystals with diameters ranging from 5 to 20 μm are dispersed throughout the fracture surface (see Figure 9d), demonstrating more numerous and smaller crystals compared to Tryptopox (see Figure 9c). These crystals could be independently grown or fragments of larger crystals that broke during the mixing process. Both fracture surfaces show characteristic patterns and flow lines that can provide insights into fracture behavior and toughening mechanisms. It is likely that toughening mechanisms such as crack bridging, particle pull-out, crack pinning, crack deflection, and crack bifurcation contribute to the thermoset's toughness, similar to previous observations in epoxy resins cured with L-tyrosine.[27] Due to the differences in crystalline fraction, the K_{IC} values of Tryptopox and Tyropox also vary significantly.

The fractured and partially pulled-out L-tryptophan crystal displays a layered structure (see Figure 9e). The surrounding smaller L-tryptophan particles appear as flow lines leading to the larger crystal. Similar layered textures are observed in L-tyrosine crystals. The smaller crystals are the result of the high shear rates ($\dot{\gamma} > 10^5\ s^{-1}$) which the suspension has to endure during three-roll milling.[25] This raises questions about the kinetics of crystal growth and the diffusion coefficients of amino acid molecules and particles before and during curing, which could be subjects for future investigations.

4 | CONCLUSION AND OUTLOOK

This investigation provides valuable insights into the mechanical properties of thermosets prepared from the aromatic amino acids L-tryptophan and L-tyrosine as curing agents for epoxy resins. Both thermosets exhibit similar glass transition temperatures, tensile strengths, flexural strengths, and compression yield strengths, indicating their comparable overall mechanical performance.

The key differentiators between Tryptopox and Tyropox lie in their Young's moduli and fracture toughness properties. The greater presence of amino acid crystals in Tyropox, likely due to the lower solubility of L-tyrosine, enhances its moduli and fracture toughness compared to Tryptopox. This suggests that amino acids, beyond serving as bio-based and latent curing agents, also act as effective toughening agents, thanks to the presence of amino acid crystals in the thermosetting matrix.

In summary, Tyropox, with its higher moduli and toughness properties, appears to be a promising candidate for use as a matrix system in prepreg production for fiber-reinforced composites. However, further research is needed to understand how the greater presence of amino acid crystals in these thermosets might impact the mechanical properties of fiber-reinforced composites, which could be the focus of future studies. This work underscores the potential of amino acids as multifunctional additives in epoxy resin systems.

AUTHOR CONTRIBUTIONS

Florian Rothenhäusler: Conceptualization (lead); data curation (lead); formal analysis (lead); investigation (lead); methodology (lead); validation (lead); visualization (lead); writing – original draft (lead). **Holger Ruckdäschel:** Project administration (lead); supervision (lead); writing – review and editing (lead).

ACKNOWLEDGMENTS

We would like to thank all colleagues of the work group "Resins & Composites" at the Department of Polymer Engineering for their support. Open Access funding enabled and organized by Projekt DEAL.

FUNDING INFORMATION

Parts of the research documented in this manuscript have been funded by the German Federal Ministry for Economic Affairs and Climate Action (BMWK) within the research project "EcoPrepregs – Grundlagenforschung zur Klärung der Struktur-Eigenschaftsbeziehungen von Epoxidharzen und Fasern aus nachwachsenden Rohstoffen zur Anwendung in der Sekundärstruktur von Flugzeugen" (grant # 20E1907A, Germany).

CONFLICT OF INTEREST STATEMENT

The authors declare no conflicts of interest.

DATA AVAILABILITY STATEMENT

The data that support the findings of this study are available from the corresponding author upon reasonable request.

ORCID

Florian Rothenhäusler https://orcid.org/0000-0001-9948-3310
Holger Ruckdäschel https://orcid.org/0000-0001-5985-2628

REFERENCES

[1] H. Schürmann, *Konstruieren mit Faser-Kunststoff-Verbunden*, Springer, Berlin **2007**.
[2] F. Henning, E. Moeller, *Handbuch Leichtbau: Methoden, Werkstoffe, Fertigung*, Carl Hanser Verlag GmbH & Company KG, Munich **2020**.
[3] H. Lengsfeld, F. Wolff-Fabris, J. Krämer, J. Lacalle, V. Altstädt, *Faserverbundwerkstoffe – Prepregs und ihre Verarbeitung*, Hanser Publishers, Munich **2014**.
[4] L. B. Bourne, F. J. M. Milner, K. B. Alberman, *Am. J. Ind. Med.* **1959**, *16*, 81.
[5] H. Greim, D. Bury, H. J. Klimisch, M. Oeben-Negele, K. Ziegler-Skylakakis, *Chemosphere* **1998**, *36*, 271.
[6] K. M. Venables, *Br. J. Ind. Med.* **1989**, *46*, 222.
[7] W. W. Anku, M. A. Mamo, P. P. Govender, *Phenolic Compounds in Water: Sources, Reactivity, Toxicity and Treatment Methods*, IntechOpen, London **2017** https://www.intechopen.com/chapters/53973
[8] P. O. Larsen, *6 – Physical and Chemical Properties of Amino Acids*, Academic Press, London **1980** https://www.sciencedirect.com/book/9780126754056/amino-acids-and-derivatives
[9] W. Leuchtenberger, K. Huthmacher, K. Drauz, *Appl. Microbiol. Biotechnol.* **2005**, *69*, 1.
[10] D. L. Nelson, M. M. Cox, *Lehninger Principles of Biochemistry*, MacMillan Learning, New York City **2021** https://www.macmillanlearning.com/college/ca/product/Lehninger-Principles-of-Biochemistry/p/1319228003
[11] Y. Li, F. Xiao, C. P. Wong, *J. Polym. Sci. Part A: Polym. Chem.* **2007**, *45*, 181.
[12] A. Motahari, A. Omrani, A. A. Rostami, *Comput. Theor. Chem.* **2011**, *977*, 168.
[13] A. Motahari, A. A. Rostami, A. Omrani, M. Ehsani, *J. Macromol. Sci. Part B: Phys.* **2015**, *54*, 517.
[14] L. Mazzocchetti, S. Merighi, T. Benelli, L. Giorgini, *AIP Conf. Proc.* **2018**, *1981*, 020170.
[15] P. Gnanasekar, N. Yan, *Polym. Degrad. Stab.* **2019**, *163*, 110.
[16] S. Merighi, L. Mazzocchetti, T. Benelli, L. Giorgini, *Processes* **2021**, *9*, 42.
[17] R. Q. Albuquerque, F. Rothenhäusler, H. Ruckdaeschel, *MRS Bull.* **2023**, *48*, 1.
[18] F. Rothenhäusler, H. Ruckdaeschel, *Polymer* **2023**, *15*, 385.
[19] A. Farkas, P. F. Strohm, *J. Appl. Polym. Sci.* **1968**, *12*, 159.
[20] R. J. Varley, *Polym. Int.* **2004**, *53*, 78.
[21] B. C. Kim, S. W. Park, D. G. Lee, *Compos. Struct.* **2008**, *86*, 69.
[22] F. Hübner, M. Hoffmann, N. Sommer, V. Altstädt, A. Scherer, T. Dickhut, H. Ruckdäschel, *Polym. Test.* **2022**, *113*, 107678.
[23] Y. Li, F. Xiao, K. Moon, C. P. Wong, *J. Polym. Sci. Part A: Polym. Chem.* **2005**, *44*, 1020.
[24] M. Shibata, J. Fujigasaki, M. Enjoji, A. Shibita, N. Teramoto, S. Ifuku, *Eur. Polym. J.* **2018**, *98*, 216.
[25] F. Rothenhäusler, H. Ruckdaeschel, *Polymer* **2022**, *14*, 4331.
[26] F. Rothenhäusler, H. Ruckdaeschel, *Polymer* **2022**, *14*, 4696.
[27] F. Rothenhäusler, H. Ruckdaeschel, *Polym. Eng. Sci.* **2023**, *63*, 4007.
[28] G. Levita, S. De Petris, A. Marchetti, A. Lazzeri, *J. Mater. Sci.* **1991**, *26*, 2348.
[29] H. Cease, P. F. Derwent, H. T. Diehl, J. Fast, D. Finley, Measurement of mechanical properties of three epoxy adhesives at cryogenic temperatures for CCD construction. 2006, 11.
[30] F. Rodante, G. Marrosu, G. Catalani, *Thermochim. Acta* **1992**, *194*, 197 https://www.sciencedirect.com/science/article/pii/004060319280018R
[31] J. G. Williams, *J. Appl. Polym. Sci.* **1979**, *23*, 3433.
[32] M. Ochi, H. Kageyama, M. Shimbo, *Polymer* **1988**, *29*, 320 https://www.sciencedirect.com/science/article/pii/0032386188903400
[33] F. G. Garcia, B. G. Soares, V. J. R. R. Pita, R. Sánchez, J. Rieumont, *J. Appl. Polym. Sci.* **2007**, *106*, 2047.
[34] I. Azuri, E. Meirzadeh, D. Ehre, S. R. Cohen, A. M. Rappe, M. Lahav, I. Lubomirsky, L. Kronik, *Angew. Chem. Int. Ed. Engl.* **2015**, *54*, 13566.
[35] V. Basavalingappa, S. Bera, B. Xue, J. O'Donnell, S. Guerin, P. A. Cazade, H. Yuan, E. U. Haq, C. Silien, K. Tao, L. J. Shimon, *ACS Nano* **2020**, *14*, 7025.
[36] D. P. Karothu, G. Dushaq, E. Ahmed, L. Catalano, S. Polavaram, R. Ferreira, L. Li, S. Mohamed, M. Rasras, P. Naumov, *Nat. Commun.* **2021**, *12*, 1326.
[37] R. Y. Adhikari, J. J. Pujols, *Nano Select* **2022**, *3*, 1314.
[38] W. Ji, B. Xue, Z. A. Arnon, H. Yuan, S. Bera, Q. Li, D. Zaguri, N. P. Reynolds, H. Li, Y. Chen, S. Gilead, S. Rencus-Lazar, J. Li, R. Yang, Y. Cao, E. Gazit, *ACS Nano* **2019**, *13*, 14477.
[39] F. Hübner, A. Brückner, T. Dickhut, V. Altstädt, A. Rios de Anda, H. Ruckdäschel, *Polym. Test.* **2021**, *102*, 107323 https://www.sciencedirect.com/science/article/pii/S0142941821002695
[40] A. Klingler, A. Bajpai, B. Wetzel, *Eng. Fract. Mech.* **2018**, *203*, 81 https://www.sciencedirect.com/science/article/pii/S0013794418300778
[41] B. B. Johnsen, A. J. Kinloch, R. D. Mohammed, A. C. Taylor, S. Sprenger, *Polymer* **2007**, *48*, 530 https://www.sciencedirect.com/science/article/pii/S0032386106012882
[42] C. B. Hübschle, M. Messerschmidt, P. Luger, *Cryst. Res. Technol.* **2004**, *39*, 274.
[43] S. Khemaissa, S. Sagan, A. Walrant, *Crystals* **2021**, *11*, 1032.

How to cite this article: F. Rothenhäusler, H. Ruckdäschel, *J. Appl. Polym. Sci.* **2024**, *141*(16), e55250. https://doi.org/10.1002/app.55250